JOURNAL OF SPACECRAFT AND ROCKETS
Vol. 41, No. 5, September–October 2004

End-to-End Optimization of Chemical-Electric Orbit-Raising Missions

David Y. Oh,* Thomas Randolph,† and Scott Kimbrel‡
Space Systems/Loral, Palo Alto, California 94303
and
Manuel Martinez-Sanchez§
Massachusetts Institute of Technology, Cambridge, Massachusetts 02139

A simple analytic multistage model is presented for combined chemical-electric orbit-raising missions. Expressions for transportation rates and optimum electric specific impulse are derived for two-stage, three-stage, variable-efficiency, and tank-limited missions of up to 100 days duration. The optimum electric specific impulse is shown to depend strongly on the specific impulse of the chemical thruster. A low-thrust-trajectory optimization model is combined with launch-vehicle performance data to derive end-to-end optimized three-dimensional chemical-electric orbit-raising profiles to geostationary orbit. Optimized profiles are derived for the Sea Launch, Ariane 4, Atlas V, Delta IV, and Proton launch vehicles. Optimum electric orbit-raising starting orbits and payload mass benefits are calculated for each vehicle. The mass benefit is shown to be between 6.1 and 7.6 kg/day with two SPT-140 thrusters, or up to 680 kg for 90 days of electric orbit raising. The optimized profiles are combined with the analytic model to a create simple parametric performance model describing multiple launch vehicles. The model is a good tool for system level analysis of electric orbit-raising missions and is shown to match calculated performance to within 13%.

Nomenclature

b	=	fitting constant
c_{lv}	=	effective launch-vehicle exhaust velocity, m/s
c_1	=	effective on board chemical thruster exhaust velocity, m/s
c_2	=	effective electric thruster exhaust velocity, m/s
c_2^*	=	optimum electric thruster effective exhaust velocity, m/s
d	=	fitting constant, m/s
g	=	9.81 m/s^2
m_0	=	spacecraft mass, beginning of orbit raising, kg
m_1	=	spacecraft mass, end of chemical orbit raising, before electric orbit raising (EOR), kg
m_2	=	spacecraft mass, end of orbit raising (payload mass), kg
$\dot{m}_2$	=	electric propulsion mass flow rate, kg/s
P	=	thruster input power, W
T_2	=	electric propulsion device thrust, N
t	=	time, s
Δv_{chem}	=	Δv for all-chemical orbit raising, m/s
Δv_{tot}	=	$\Delta v_1 + \Delta v_2$
Δv_1	=	Δv for chemical portion of a C-EOR mission, m/s
Δv_2	=	Δv for electric portion of a C-EOR mission, m/s
$\Delta v_{2\text{eff}}$	=	chemical Δv effectively replaced by electric Δv, m/s
η_p	=	thruster efficiency
η_v	=	mission planning efficiency

Received 13 December 2001; revision received 11 August 2003; accepted for publication 11 August 2003.

*Principal Engineer, Systems Engineering; currently Senior Engineer, Deep Space Mission Architecture Group, Jet Propulsion Laboratory, California Institute of Technology, 4800 Oak Grove Drive, M/S 301-170S, Pasadena, CA 91109-8099; david.y.oh@jpl.nasa.gov. Member AIAA.

†Senior Engineering Specialist, Propulsion Engineering. Senior Member AIAA.

‡Systems Engineer, Systems Engineering.

§Professor, Department of Aeronautics and Astronautics. Senior Member AIAA.

Introduction

WESTERN commercial communications satellites are generally launched into a transfer orbit and then boosted into geostationary orbit (GEO) using an onboard chemical propulsion system (OBS). This is referred to as orbit raising. Commercial manufacturers are now using electric propulsion for orbit raising.[1–3] Electric orbit raising (EOR) occurs over a period of days or months and can save hundreds of kilograms of mass. Although it is possible to accomplish all of orbit raising using EOR, the time required (many months) is prohibitive for current commercial applications. Combined chemical-electric missions (C-EOR) provide customers with significantly greater payload capacity and yet maintain an acceptable on-orbit delivery time. From the point of view of the satellite owner, optimization of the mission requires maximizing the dry mass benefit per day of EOR, or transportation rate. When the power available for EOR is fixed, there is an inverse relationship between thrust and specific impulse I_{sp}, and there is an optimum I_{sp} that maximizes transportation rate.

This paper describes a simple analytic model that treats orbit raising as a series of chemical/electric stages. The model is used to derive a modified form of the rocket equation and to determine the theoretical optimum I_{sp} for C-EOR missions. Complex issues associated with low-thrust-trajectory optimization are summarized in single parameter, a mission planning efficiency, which is independently calculated for each trajectory. A numerical-graphical optimization method is used to generate end-to-end optimized C-EOR mission profiles for orbit raising to GEO. The method optimizes the overall performance of the launch vehicle, chemical OBS, and electric propulsion system. Planning efficiencies are calculated for each trajectory, and multistage analytic models are applied to each launch vehicle. These results are combined to create a simple parametric model that can be used to calculate transportation rates and optimum I_{sp} for a variety of vehicles. The model is a good tool for system level analysis of electric orbit-raising missions and for trade studies involving different types of electric thrusters.

Previous Work

It is well known that for electric propulsion systems there is a tradeoff between propellant mass and power system mass that results in an optimum specific impulse I_{sp} that maximizes payload

mass.[4] However, on commercial missions time has an inherent cost that must be considered in the optimization. The aim of the mission planner is to minimize this cost by maximizing transportation rate (kilograms gained/time) rather than overall payload dry mass. In the past, derivations have been made for the I_{sp} that maximizes transportation rate as a function of specific power (watts/kilogram).[5] These derivations assume that the power system imposes a mass penalty that varies with power level. On commercial missions substantial payload power is available for "free" during orbit raising that can be used without cost or mass penalty. The optimizations presented in this paper reflect the requirements of commercial missions by optimizing transportation rate at a fixed power level.

Considerable previous work has been done on the optimization of low-thrust missions of all types, including orbit raising.[6–9] Much of this work has focused on the low-thrust portion of the mission and has ignored or simplified the chemical stages. Although this approach is appropriate for missions dominated by electric propulsion (such as deep-space missions), near-term commercial EOR missions are dominated by the launch vehicle and the chemical OBS. For this reason, it is important to optimize usage of the chemical stages as part of the overall C-EOR mission. This paper will demonstrate the strong relationship between the chemical and electric stages and show that the optimum electric I_{sp} depends directly on the I_{sp} of the chemical stages.

The Solar Electric Propulsion Steering Program for Optimal Trajectories (SEPSPOT) has a limited capability to jointly optimize the chemical-electric stages of an orbit-raising mission and has been used to calculate optimum EOR starting orbits to GEO for various launch vehicles.[10] SEPSPOT contains a simple staging model that assumes the spacecraft begins in a circular orbit and has a single high-thrust chemical stage. This assumption is unrealistic because it does not consider the possibility of using the launch vehicle's upper stage to reach elliptical separation orbits. This paper derives optimized trajectories that fully account for the performance of the launch vehicle to all practical separation orbits.

Analytic Chemical-Electric Staging Models

Two-Stage C-EOR Model

In this section expressions are derived for the payload mass delivered to orbit and the optimum electric specific impulse for a two-stage C-EOR mission. The expressions assume that the efficiency of the electric propulsion device is constant at all thrust levels.

Figure 1a shows a simplified representation of an all-chemical orbit-raising mission in which the spacecraft begins with an initial mass M_0, is accelerated through a velocity change ΔV_{chem} and ends with payload mass M_2. Figure 1b shows a C-EOR mission that has been divided into two parts, a chemical stage with velocity change Δv_1 and an electric stage with velocity change Δv_2. The spacecraft begins with an initial mass M_0, ends the chemical phase of the mission with a mass M_1, and ends orbit raising with a final mass M_2. The mass fraction for each phase of the mission is given by the rocket equation:

$$m_1/m_0 = e^{-\Delta v_1/c_1} \tag{1}$$

$$m_2/m_1 = e^{-\Delta v_2/c_2} \tag{2}$$

EOR missions require more Δv than chemical missions because the low thrust level does not allow the use of impulsive burns, and so the sum of Δv_1 and Δv_2 is greater than Δv_{chem}. It is useful to define Δv_{2eff} to represent the amount of chemical Δv replaced by electric orbit raising. An efficiency factor relates Δv_{2eff} to Δv_2:

$$\Delta v_{2eff} \equiv \Delta v_{chem} - \Delta v_1 \tag{3}$$

$$\eta_v \equiv \frac{\Delta v_{2eff}}{\Delta v_2} \tag{4}$$

where η_v represents the effectiveness of the EOR thrust trajectory and steering profile. Combining Eqs. (2) and (4) gives the following form of the rocket equation:

$$m_2/m_1 = e^{-\Delta v_{2eff}/\eta_v c_2} \tag{5}$$

The planning efficiency is a penalty applied to the electric thruster's exhaust velocity because the spacecraft is not flying an impulsive mission profile. Three more expressions relate power, time, thrust, and mass flow rate to the rocket equation:

$$P = \tfrac{1}{2}\dot{m}_2 c_2^2 \big/ \eta_p \tag{6}$$

$$m_2 = m_1 - \dot{m}_2 t \tag{7}$$

$$T_2 = \dot{m}_2 c_2 \tag{8}$$

Initially, we make the following assumptions: 1) a fixed amount of power is available for EOR, 2) a fixed amount of time is available for EOR, 3) the electric propulsion (EP) device is always on (no coast periods), and 4) the EP device's I_{sp} is fixed throughout the mission. The first two assumptions are functions of the design of the spacecraft and the target on-orbit delivery date. Fixing time ensures that maximizing delivered mass will also maximize transportation rate. The final two assumptions are typical for minimum-time-to-orbit EOR missions. Combining Eqs. (1), (3), and (5–7) gives the overall rocket equation for a C-EOR mission:

$$e^{-\Delta v_{chem}/c_1} = \frac{m_2}{m_0}\left(\frac{\eta_p P t}{\frac{1}{2}m_2 c_2^2} + 1\right)^{(1-\eta_v c_2/c_1)} \tag{9}$$

Equation (9) is similar to the standard rocket equation but with an additional term that captures the benefits of EOR. Two parameters, Δv_{chem} and η_v, must be calculated computationally based on an assumed EOR steering profile. Time, power, and thruster efficiency are all equivalent parameters in Eq. (9), and so a 10% increase in EOR duration has exactly the same effect as a 10% increase in EOR power. This is to be expected because with fixed I_{sp} the total impulse delivered scales linearly with all three parameters.

Expressions for the transportation rate and optimal specific impulse are derived by combining Eqs. (1), (3), (5), and (7) to obtain

$$m_0/m_1 = (1 - \dot{m}_2 t/m_1)^{(\eta_v c_2/c_1)} e^{\Delta v_{chem}/c_1} \tag{10}$$

Expanding Eq. (10) as a Taylor series and neglecting higher-order terms,

$$\frac{m_0}{m_1} = \left(1 - \frac{\eta_v c_2 \dot{m}_2 t}{c_1 m_1}\right) e^{\Delta v_{chem}/c_1} \tag{11}$$

This linearization is valid when

$$(\eta_v c_2/c_1 - 1)(\dot{m}_2 t/2m_1) \ll 1 \tag{12}$$

The term in parentheses is generally of order $0.1 \sim 1$, so as long as the electric propellant mass is small compared to the spacecraft mass the linearization is valid. Substituting Eqs. (7) and (8) into

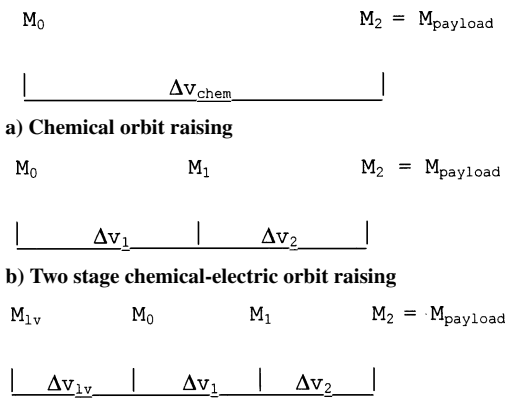

Fig. 1 Simple model of chemical-electric orbit-raising missions.

Eq. (11), solving for payload mass, and taking the time derivative gives an expression for the transportation rate:

$$\frac{\mathrm{d}m_2}{\mathrm{d}t} = \frac{\eta_v T_2}{c_1} - \frac{T_2}{c_2} \tag{13}$$

This derivation assumes the mission planning efficiency is constant with respect to flight time, an assumption that will be justified in the second half of this paper. The term η_v is determined by the spacecraft's starting orbit, ending orbit, and thrust steering profile. Exact values are calculated in the second half of this paper and are shown to be relatively constant for missions of short duration (90 days or less). Substituting Eqs. (6) and (8) into Eq. (13), taking the derivative with respect to c_2, and setting the result equal to zero gives the optimal exhaust velocity:

$$c_2^* = 2c_1/\eta_v \tag{14}$$

The optimum exists because at fixed power there is a trade between the mass benefit, maximized by a high specific impulse, and transit time, minimized by a high thrust. The exact value of c_2^* depends on the chemical thruster's exhaust velocity because total impulse delivered by the EP device displaces fuel from the chemical thruster at a ratio that depends on the flight trajectory, steering profile, and planning efficiency η_v. An interesting result in Eq. (14) is that c_2^* is insensitive to specific power. This implies that on short-duration commercial missions an optimal electric thruster exhaust velocity can be selected without regard to the spacecraft power level or specific power parameter. Power and time do not appear in Eq. (14) because of the linearization done to derive Eq. (11). Equation (9) can be differentiated to give an implicit expression for the optimum electric I_{sp} valid for missions of arbitrary duration. The result is

$$4Pt\eta_p\left(1 - \frac{\eta_v c_2}{c_1}\right) + \frac{\eta_v c_2}{c_1}\left(2Pt\eta_p + c_2^2 m_2\right)\ell_n\left(\frac{2Pt\eta_p}{m_2 c_2^2} + 1\right) = 0 \tag{15}$$

Variable Thrust Efficiency Model

In the preceding section it was assumed that the efficiency of the electric thruster is constant at all thrust levels. In this section the efficiency is allowed to vary with exhaust velocity in a manner typical for Hall and ion thrusters. The efficiency curve for these devices can be approximated by the function

$$\eta_p = bc^2/(c^2 + d^2) \tag{16}$$

where b and d are thruster specific constants derived from fits to laboratory data.[11] For this analysis two efficiency profiles are considered: one for a Hall thruster and one for an ion thruster derated to operate at low I_{sp}. An SPT-140 is used to represent a typical Hall thruster. Its efficiency curve is derived by fitting Eq. (16) to laboratory data at constant power.[12] The fit shows good agreement in the range 1650–2800 s and does not include the thruster's separate magnet supply. A fit for a derated ion thruster is taken from Oleson.[13] This fit is not based on constant power data. Figure 2 shows the resulting efficiency curves and Table 1 gives corresponding fitting parameters.

A C-EOR rocket equation, which accounts for variable thrust efficiency, is derived by substituting Eq. (16) into Eq. (9):

$$e^{-\Delta v_{\mathrm{chem}}/c_1} = \frac{m_2}{m_0}\left[\frac{bPt}{\frac{1}{2}m_2\left(c_2^2 + d^2\right)} + 1\right]^{(1-\eta_v c_2/c_1)} \tag{17}$$

Table 1 Thruster efficiency curve-fitting parameters

Thruster	b	d, m/s
SPT-140	0.684	7,998
Ion thrusters	0.825	14,570

Table 2 Theoretical optimum I_{sp} for C-EOR missions

Thruster type	Optimum I_{sp}
Fixed efficiency thruster ($\eta_v = 0.5$)	1250 s
SPT-140 Hall thruster	1645 s
Derated ion thruster	2230 s

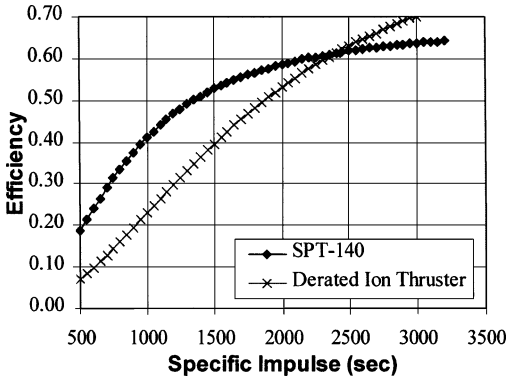

Fig. 2 Thruster efficiency vs specific impulse (Hall and ion thrusters).

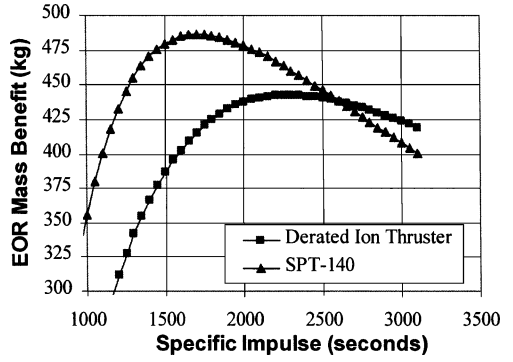

Fig. 3 EOR mass benefit vs specific impulse for Hall and ion thrusters.

This expression is linearized and expanded when time is small:

$$e^{-\Delta v_{\mathrm{chem}}/c_1} = \frac{m_2}{m_0} + \frac{2bPt}{m_0\left(c_2^2 + d^2\right)} - \frac{2\eta_v bPtc_2}{m_0 c_1\left(c_2^2 + d^2\right)} \tag{18}$$

Differentiating implicitly and setting the derivative equal to zero gives

$$c_2^* = c_1/\eta_v \pm \sqrt{c_1^2/\eta_v^2 + d^2} \tag{19}$$

The corresponding optimum Hall- and ion-thruster specific impulses are calculated using the positive root. Table 2 compares values computed using Eq. (19) with that computed using the fixed efficiency Eq. (14).

The ion thruster has a higher optimum than the Hall thruster because it is relatively inefficient at high thrust levels. A comparison of the mass benefit from these devices is calculated using Eq. (17) and shown in Fig. 3. In this figure $P = 10$ kW, $t = 90$ days, $M_0 = 6000$ kg, $\Delta v_{\mathrm{chem}} = 1.8$ km/s, and $\eta_v = 0.5$.

With the efficiency curves defined in Table 1, the Hall thrusters provide about 10% better mass performance than the ion thrusters when both devices are operated at their optimum I_{sp}. The optimum Hall-thruster operating point is near the nominal operating point for existing devices that are designed to provide sufficient lifetime for EOR.[14,15] The optimum ion-thruster operating point is lower than is typical for existing ion thrusters. The slope of the curve in Fig. 3 is relatively steep below the optimum point and relatively flat above it. As a result, it is might be better to optimize the life of the ion thruster

by operating at a higher specific impulse of 3000 s and accept some mass performance penalty.

Three-Stage Derivation

A fully optimized C-EOR mission must jointly optimize all elements of the system: the OBS, the electric thruster, and the launch vehicle. When modeling the end-to-end mission profile, it is sometimes useful to treat the launch vehicle as a unique "chemical stage" that fires before the OBS. In this section we derive the rocket equation and optimum specific impulse for a three-stage C-EOR mission with two chemical stages and one electric stage. The resulting three-stage model will be used to model the performance of the Sea Launch vehicle in the final section of this paper.

Figure 1c shows the three-stage-model mission profile. The spacecraft begins with an initial mass M_{lv}. This mass is defined as the launch-vehicle's separated mass capability to a relatively low subsynchronous apogee reference orbit. The effective launch vehicle Δv (Δv_{lv}) is defined as the velocity change required to transfer from this reference orbit to the true separation orbit. This stage ends with launch vehicle's true separation mass M_0. M_0 is also the starting mass for the satellite's OBS. The mass fraction for the first chemical stage is given by the following rocket equation:

$$m_0/m_{\text{lv}} = e^{-\Delta V_{\text{lv}}/c_{\text{lv}}} \tag{20}$$

Equation (3) now takes the form

$$\Delta v_{2\text{eff}} = \Delta v_{\text{chem}} - \Delta v_1 - \Delta v_{\text{lv}} \tag{21}$$

The term Δv_{lv} can be derived from data in the launch-vehicle user's guides. This effective velocity is much lower than the actual exhaust velocity of the upper stage because it implicitly incorporates the mass penalty associated with the weight of the empty upper stage as well as any inefficiencies in the powered launch trajectory.

To derive expressions for optimum electric specific impulse and transportation rate, it is necessary to make an assumption about the distribution of Δv between the launch vehicle and OBS. In the Sea Launch case, which uses spiral EOR, Δv_1 varies from 1466 m/s for a GEO apogee to 1430 m/s at a 20,000-km apogee. This variation is small compared to the variation of 395 m/s in Δv_{lv} and 813 m/s in Δv_2, respectively. If it is assumed that Δv_1 is constant over the range of mission considered, the following expression is obtained:

$$m_{\text{lv}}/m_0 = (1 - \dot{m}_2 t/m_1)^{(\eta_v c_2/c_{\text{lv}})} e^{\Delta v_{\text{chem}}/c_{\text{lv}}} e^{-\Delta v_1/c_{\text{lv}}} \tag{22}$$

Expanding Eq. (22) as a Taylor series and neglecting second-order and higher terms,

$$\frac{m_{\text{lv}}}{m_0} = \left(1 - \frac{\eta_v c_2 \dot{m}_2 t}{c_{\text{lv}} m_1}\right) e^{\Delta v_{\text{chem}}/c_{\text{lv}}} e^{-\Delta v_1/c_{\text{lv}}} \tag{23}$$

Again, the linearization is valid when the electric propellant mass is small compared to the spacecraft mass.

Inserting Eqs. (1), (7), and (8) into Eq. (23) and taking the time derivative produces an analytic expression for the transportation rate:

$$\frac{\mathrm{d}m_2}{\mathrm{d}t} = \frac{\eta_v T_2}{c_{\text{lv}}} - \frac{T_2}{c_2} \tag{24}$$

This derivation assumes that the launch-vehicle's effective exhaust velocity is constant. These assumptions are applicable to the optimized Sea Launch mission discussed later in this paper. Substituting Eqs. (6) and (8) into Eq. (24) and taking the derivative with respect to c_2 provides the optimal exhaust velocity:

$$c_2^* = 2c_{\text{lv}}/\eta_v \tag{25}$$

This expression is identical to Eq. (14) except the chemical exhaust velocity has been replaced by the effective launch-vehicle exhaust velocity. It is valid when the thrust efficiency is constant with respect to electric exhaust velocity.

Tank-Limited Derivation

When working with preexisting spacecraft configurations, it is useful to consider cases where the chemical propellant tank size is fixed by design or where spacecraft volume is limited. In the case of fixed chemical propellant mass, the transportation rate and optimal exhaust velocity equations take different forms. It is necessary to introduce the equation for chemical propellant mass:

$$m_{\text{cp}} = m_1 - m_0 \tag{26}$$

Inserting Eqs. (7) and (26) into Eq. (11), solving for payload mass, and taking the time derivative produces an analytic expression for the transportation rate:

$$\frac{\mathrm{d}m_2}{\mathrm{d}t} = \frac{\eta_v T_2}{c_1\left(1 - e^{-\Delta v_{\text{chem}}/c_1}\right)} - \frac{T_2}{c_2} \tag{27}$$

This derivation is subject to the same assumptions as Eq. (13) but will typically result in much higher values for the transportation rate. In this chemical-propellant-limited case EOR can take advantage of additional unused launch-vehicle capacity, resulting in greater performance improvements.

Substituting Eqs. (6) and (8) into Eq. (27), taking the derivative with respect to the electric specific impulse, and setting the equation to zero provides the optimal exhaust velocity:

$$c_2 = (2c_1/\eta_v)\left(1 - e^{-\Delta v_{\text{chem}}/c_1}\right) \tag{28}$$

This expression will typically result in much smaller values for the optimal exhaust velocity (i.e., higher thrust) than Eq. (14).

End-to-End Optimizations

In the preceding section basic multistage performance models were derived for C-EOR missions based on the assumption that the mission planning efficiency is constant. In this section the planning efficiency is calculated for end-to-end optimized C-EOR missions on multiple launch vehicles. The result validates the assumption that mission planning efficiency is constant for short-duration C-EOR missions. The section begins with a two-dimensional end-to-end mission optimization using the Sea Launch vehicle. The optimization method is validated through comparison to previously published results. The end-to-end optimization method is then extended to three dimensions to cover multiple launch vehicles.

Two-Dimensional End-to-End Optimization

A two-dimensional optimization of a C-EOR mission to GEO is conducted by combining a simple Sea Launch performance model with a low thrust optimizer developed by Kimbrel.[16] As before, the objective of the optimization is to maximize transportation rate. To simplify the analysis, the following assumptions are made: 1) a fixed amount of power is available for EOR; 2) the EP device is always on (no coast periods); 3) the EP device's I_{sp} and thrust are constant throughout the mission; 4) the launch-vehicle separation orbit is identically zero inclination; 5) external tidal/multibody perturbation effects are neglected; 6) orbit phasing (aiming for a particular final longitude) is neglected; and 7) there is no limit on fuel tank size onboard the satellite. Because the EP device is always on, minimizing electric ΔV maximizes both payload mass and transportation rate. Because Sea Launch has a restartable upper stage, it can inject its payload into a range of orbits of near zero inclination. We begin by considering missions in which the satellite is injected directly into its EOR starting orbit and has no chemical OBS.

The end-to-end optimization uses a combination of graphical and numerical optimization methods. The low-thrust optimizer is used to generate a contour map of the electric Δv required to reach GEO as a function of starting eccentricity and semimajor axis. It begins with the standard orbital perturbation equations and does a two-step optimization using LaGrange multipliers. The first step optimizes the steering profile within each orbit to achieve the desired change in orbital elements with minimum ΔV. The second step uses the orbit averaged equations to optimize the overall path to GEO. The

Table 3 Typical thruster performance parameters

Thruster	Thrust, N	I_{sp}, s	Power, W
Biprop[18]	445	322	N/A
SPT[12]	0.288	1780	4500
XIPS[19]	0.165	3500	4500

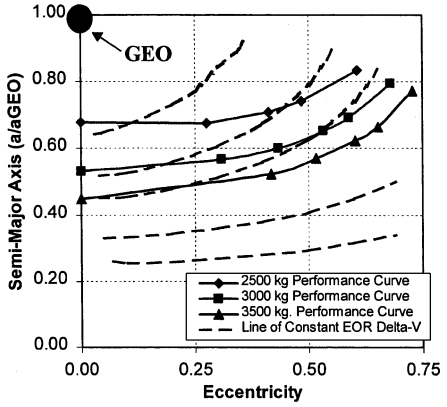

Fig. 4 Sea Launch performance overlaid on contours of constant electric ΔV.

optimization is done numerically using methods described in detail in Ref. 16. Launch-vehicle performance curves are superimposed on the contour map, and the result is examined to graphically determine the optimum EOR starting orbit. For a given separated mass the objective is to find the starting orbit that requires the least electric ΔV (and therefore the shortest time) to reach GEO.

A typical Sea Launch contour map is shown in Fig. 4. The EOR ΔV contours are shown as dotted lines, each of which is a group of starting orbits that require the same EOR ΔV, and therefore the same amount of time, to reach GEO. Launch-vehicle performance curves are taken from Ref. 17 and assume direct injection into the EOR starting orbit. Each curve is a family of orbits to which Sea Launch can deliver a given separated mass. The target orbit is $a/a_f = 1$ and $e = 0$.

The mission tradeoffs can be clearly seen in Fig. 4. The launch vehicle delivers better performance to eccentric separation orbits, but EOR delivers better performance from circular starting orbits. In this case the benefit in EOR performance outweighs the penalty in launch vehicle performance, and so it is best to start in a circular orbit. The optimum EOR thrust profile is spiral orbit raising, in which the satellite's orbit is always circular and the thrust vector is always directed along the velocity vector.

Once the optimum EOR starting orbit is identified, the planning efficiency, EOR mass benefit, and transportation rate can be directly calculated at a given thrust and power level. Typical performance characteristics for onboard chemical and electric thrusters are shown in Table 3 (Refs. 12, 18, and 19).

Although we have assumed a direct injection to EOR, conceptually a chemical OBS acts as an extra stage for the launch vehicle. As a result, the optimum starting orbit for EOR with the chemical OBS should be the same as in the direct-injection case, giving the orbit-raising profile shown in Fig. 5.

A spreadsheet is used to calculate the transportation rate and planning efficiency for the mission profile shown in Fig. 5 assuming the use of two SPT-140 thrusters for EOR and a bipropellant OBS with performance shown in Table 3. The result is a nearly constant mass benefit of 7.5 kg/day, or 675 kg over 90 days of EOR. The calculated planning efficiency is shown in Fig. 6 and varies little with EOR duration for missions less than 90 days duration. This verifies that the planning efficiency can be assumed constant when deriving multistage C-EOR performance models for two-dimensional missions.

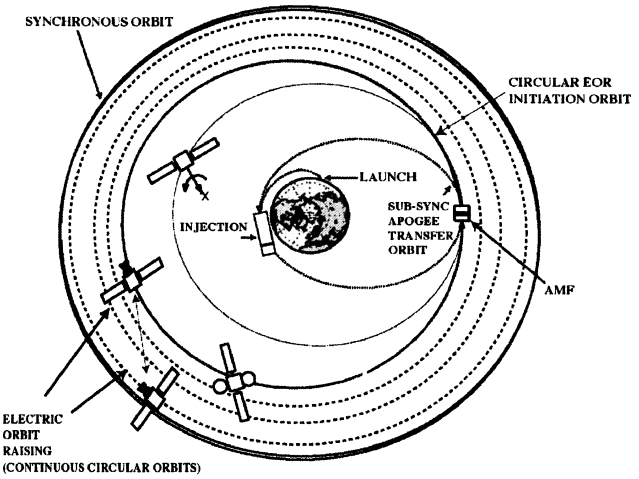

Fig. 5 Transportation rate optimized Sea Launch C-EOR mission: AMF = apogee motor firing.

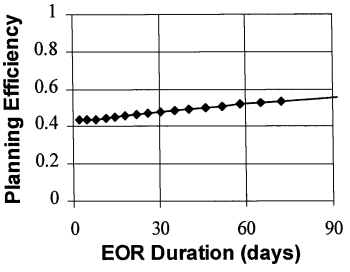

Fig. 6 Sea Launch planning efficiency vs EOR duration.

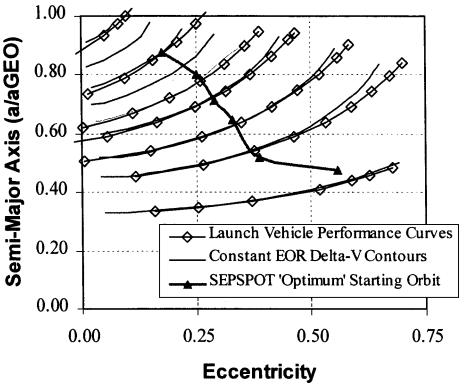

Fig. 7 Circular LEO starting orbit performance overlaid on contours of constant electric ΔV.

Verification and Comparison to Previous Work

To verify the accuracy of the graphical optimization method, a comparison was made between optimum orbits calculated using the methods just described and SEPSPOT-generated optimum orbits previously reported in the literature.[10] SEPSPOT's end-to-end optimization capability is limited to a single high-thrust stage with a circular starting orbit. As a result, SEPSPOT cannot directly simulate an elliptical separation orbit from the launch vehicle. Instead, the launch vehicle is assumed to place the satellite and its OBS into a low-altitude circular parking orbit. To study the effects of this assumption, the graphical optimization method was applied to a satellite with a chemical OBS that starts in a zero-inclination 200-km-altitude circular orbit. The separated mass is arbitrarily assumed to be 5000 kg, and the OBS specific impulse is approximately 320 s. A two-burn transfer is used to reach an EOR starting orbit between LEO and GEO. Chemical stage performance curves are calculated by varying the OBS burns to generate lines of constant EOR starting mass. The results are shown in Fig. 7. Also shown are optimum Sea Launch EOR starting orbits calculated using SEPSPOT, as derived from data presented in Ref. 10.

The results in Fig. 7 differ significantly from those in Fig. 4. Although difficult to see, for each mass curve in Fig. 7 there is a shallow minimum where the OBS performance curve is tangent to an EOR ΔV contour. The optimum starting orbits identified by SEPSPOT generally lie close to these minimum points when a/a_{GEO} is greater than 0.5. The match is close enough to validate the graphical optimization method in this regime. When a/a_{GEO} is less than 0.5, SEPSPOT favors an elliptical orbit in order to avoid solar-array degradation caused by the Earth's radiation belts. The graphical method does not optimize for radiation degradation and therefore gives a different answer in this regime. These results both confirm the accuracy of the graphical method and also demonstrate its limitations at low-altitude starting orbits. Commercial C-EOR missions of less than 90 days duration operate at high altitudes where radiation degradation is not a major factor in the optimization.

The differing results of Figs. 4 and 7 are explained by considering the different initial conditions used to generate the two plots. SEPSPOT's limitations require an assumption that the launch vehicle uses a circular starting orbit. Figure 4 is based on actual Sea Launch performance curves and therefore accounts for the true performance of the vehicle to elliptical orbits. Staging effects further complicate the optimization by changing the relative efficiency of apogee and perigee burns. The graphical optimization method models the true performance of the launch vehicle and is therefore more accurate than SEPSPOT when optimizing the Sea Launch end-to-end C-EOR mission to GEO.

One advantage of the graphical method is that it provides information about the sensitivity of the optimization. When starting from a circular orbit, the chemical stage performance curves nearly overlap the EOR ΔV contours, resulting in very shallow minima. Because the minima are shallow, as additional constraints are added to the optimization, a numerical optimizer might have trouble converging on the optimum EOR starting orbit. Figure 7 shows that, in general, when starting from LEO overall mass performance is basically insensitive to EOR starting orbit.

Three-Dimensional End-to-End Launch-Vehicle Optimization

This section describes methods used to derive optimized C-EOR mission profiles for the Ariane 4, Atlas V, Delta IV, and Proton launch vehicles. These vehicles do not launch from the Equator, and so another dimension, inclination change, is included in the analysis. The basic assumptions are the same as in the two-dimensional case with the following changes and additions: 1) the launch-vehicle separation orbit is a fixed nonzero inclination; 2) perigee velocity augmentation burns (PVA) using the OBS are not allowed; and 3) the geometry of the low-thrust portion of the mission is restricted to orbits where the line of apsides and line of nodes are colinear (i.e., apogee and perigee are at the nodes). PVAs are low-altitude perigee burns conducted using the OBS. They are operationally inconvenient and are excluded in this analysis. Launch-vehicle performance is estimated at different apogees and inclinations by extrapolating data in the user's guides. Launch-vehicle performance curves are calculated at a given separation inclination using data from the user's guides.[20–23] The separation orbit inclination is chosen to optimize the performance of the launch vehicle and is generally close to the latitude of the launch site. An exception is the Proton, which has a restartable upper stage that fires at apogee to raise perigee and lower inclination prior to separation.[23] A separation inclination of 30 deg was used with this vehicle, the highest inclination for which GTO orbit performance is reported in the user's guide. In practice, large satellites might not be able to use high-inclination separation orbits because of fuel tank volume limitations. Tank size limits are ignored in both the two- and three-dimensional optimizations. The significance of this assumption is discussed further at the end of this paper.

For each vehicle an all-chemical orbit-raising mission is defined as a reference baseline. This mission consists of a geosynchronous transfer orbit (GTO) injection followed by an apogee burn from the OBS. Because the apogee of the separation orbit is coincident with the line of nodes, a single burn can be used to raise perigee and to change inclination. This is the most efficient configuration for conventional chemical orbit raising, and it is expected that it will be close to the most efficient configuration for C-EOR missions because the majority of the ΔV for orbit raising is provided by the launch vehicle and chemical OBS. This geometry is also consistent with geometric restrictions required by the three-dimensional low-thrust optimizer used for this study. Because of the restartable upper stage, the separation perigee with Proton is considerably higher than perigee with other launch vehicles. Otherwise, its reference all-chemical mission profile is similar to that of other launch vehicles.

The electric ΔV required to reach GEO was calculated using a numerical low-thrust optimizer called MITEOR3D, which is described in detail Ref. 16. This program uses a two-step optimizer very similar to that used in the two-dimensional case, but optimizes the steering profile in three dimensions. To simplify the analysis, the optimizer assumes that the line of apsides and line of nodes are coincident at the start and end of orbit raising. The steering profiles are self-consistent and maintain the initial orientation of the line of apsides relative to the line of nodes. In practice, perturbations, steering errors, and other factors can disturb this geometry. Although this introduces some errors, the constant EOR ΔV contours are generally smooth, so that small perturbations should have little effect on overall mass performance.

The range of starting orbits considered was limited by the allowable EOR duration to inclinations less than 5 deg. Contour plots of electric ΔV were created, and chemical stage performance curves were superimposed on the plots to determine which starting orbits require the least electric ΔV to reach GEO. The performance curves account for both the performance of the launch vehicle and for the performance of the chemical OBS. EOR starting orbit inclination was varied parametrically to determine what inclination gives the best performance for a given mission duration.

Figure 8 shows EOR ΔV contours overlaid on lines of constant EOR starting mass for an Atlas V 401 with an initial separation inclination of 27 deg and EOR starting inclination of 3 deg. The launch-vehicle/OBS performance lines have been spaced so the optimum EOR starting orbit is near the intersection of the performance lines and the EOR contours. The optimum orbits are elliptical and slightly supersynchronous. The higher apogee enhances the performance of the OBS, which is changing the orbit's inclination by 24 deg. Figure 9 shows an equivalent plot for an Ariane 44L vehicle. Here, the launch-vehicle's separation orbit is 7 deg, and the starting EOR inclination is 1 deg.

The optimum starting orbits in Fig. 9 are more circular than those in Fig. 8 and have subsynchronous apogees. Because Ariane launches from a lower latitude than Atlas, the OBS is doing only 6 deg of inclination change. The optimization therefore tends to favor spiral EOR over an elliptical transfer. The optimum orbits for a Delta IV Heavy vehicle are similar to those for an Atlas, but, as shown in Fig. 10, the optimum orbits for the Proton M/Breeze M have a fundamentally different character because of the vehicle's unique flight profile.

The standard Proton M/Breeze M uses a restartable upper stage to launch to a fixed apogee (GTO) with a variable perigee and inclination. The OBS further raises perigee and changes inclination

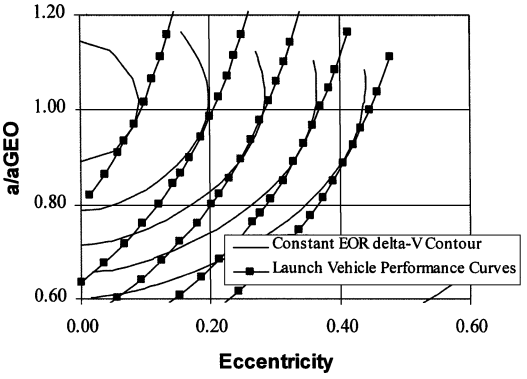

Fig. 8 Atlas V 401 performance overlaid on contours of constant electric ΔV (27-deg inclination separation orbit, 3-deg EOR starting orbit).

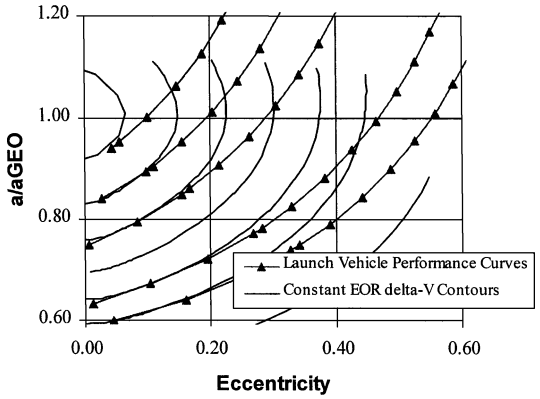

Fig. 9 Ariane 44L performance overlaid on contours of constant electric ΔV (7-deg separation orbit, 1-deg EOR starting orbit).

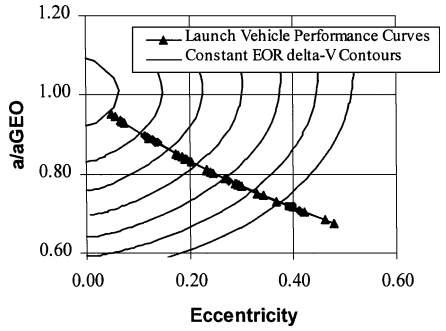

Fig. 10 Proton M/Breeze M performance curves overlaid on contours of constant electric ΔV (30-deg inclination separation orbit, 1-deg EOR starting orbit).

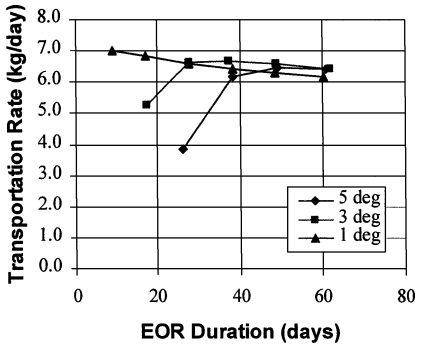

Fig. 11 Atlas V 401 EOR transportation rate vs EOR duration and starting inclination (27-deg inclination separation orbit).

but leaves apogee fixed. As a result, the allowable family of EOR starting orbits lies on a line in Fig. 10. Each EOR starting mass has a separate optimum on this line. Supersynchronous and subsynchronous transfer orbits were not considered because of the limited data available in the user's manual. Different optimum orbits might result if these separation orbits are considered.

For each launch vehicle optimum EOR starting orbits were identified, and planning efficiencies, EOR mass benefit, and transportation rate were calculated as a function of inclination. The results assume the use of two SPT-140 thrusters for orbit raising. Figures 11 and 12 show transportation rate and planning efficiency as a function of EOR starting inclination for the Atlas V 401. As one would expect, for short-duration missions it is necessary to start EOR at a low inclination. As EOR duration increases, the optimum starting inclination also increases, creating a family of EOR starting orbits. Looking at the peak of each curve, the optimum transportation rate and planning efficiency are relatively constant for short-duration missions. This verifies that the planning efficiency can be assumed constant

Table 4 Launch-vehicle modeling characteristics

Launch vehicle	Planning efficiency	Type of model	Effective chemical I_{sp}, s	Simple model, kg/day	Actual value, kg/day
Sea Launch	0.484	Three stage	240	7.38	7.6
Ariane 44L	0.550	Two stage	322	5.82	6.3
Delta 4H	0.630	Two stage	322	7.08	6.2
Atlas 401	0.644	Two stage	322	7.30	6.7
Proton M/Breeze M	0.607	Two stage	322	6.72	6.2

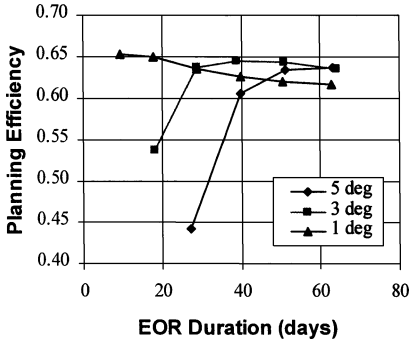

Fig. 12 Atlas V 401 planning efficiency vs EOR duration and starting inclination (27-deg inclination separation orbit).

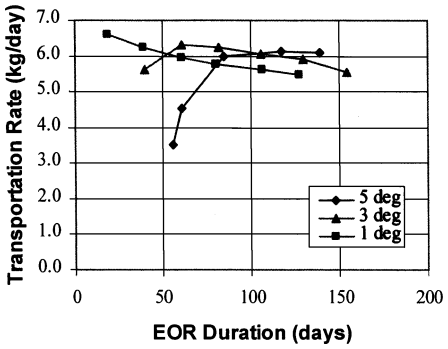

Fig. 13 Delta 4H EOR transportation rate vs EOR duration (28.5-deg inclination separation orbit).

when applied to short duration three-dimensional orbit-raising missions.

Figure 13 shows calculated transportation rates for a Delta IV Heavy (Delta 4H) launch vehicle. Figures 14 and 15 show the same parameters for an Ariane 44L and Proton M/Breeze M. Overall, the calculated transportation rates fall in a fairly narrow range, between 5.5 and 6.5 kg/day. Table 4 shows the mean planning efficiency calculated for each vehicle. The planning efficiency lies between approximately 0.45 and 0.60. It grows slightly as launch latitude increases. The overall transportation rate varies less with launch latitude. For missions of 90 days duration, the payload mass benefit is between 500 and 585 kg, a benefit large enough to be economically attractive to a commercial satellite customer.[24]

Application of Two- and Three-Stage Models

For system-level analysis it is desirable to incorporate the performance of the trajectories shown in the preceding section into a single simple model. In this section analytic multistage models are used to develop a simple parametric performance model that applies to C-EOR missions to GEO with multiple launchers. Two- and three-stage versions of Eq. (13) can be used to estimate EOR transportation rates for different launch vehicles. The results are summarized in Fig. 16 and Table 4. The bars marked actual value in Fig. 16 show the average transportation rate as calculated directly for each launch vehicle using the optimized trajectories identified in the preceding section. Launch-vehicle performance is taken from the

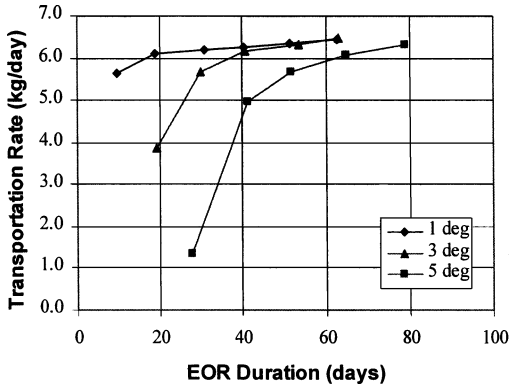

Fig. 14 Ariane 44L transportation rate vs EOR duration (7-deg separation orbit).

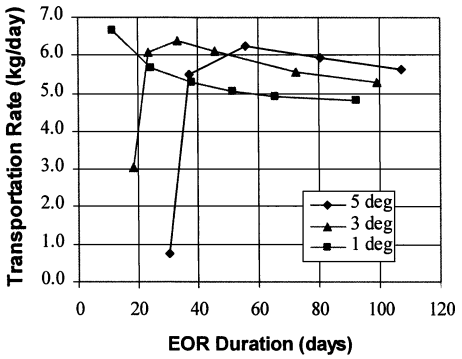

Fig. 15 Proton M/Breeze M EOR transportation rate vs EOR duration (30-deg inclination separation orbit).

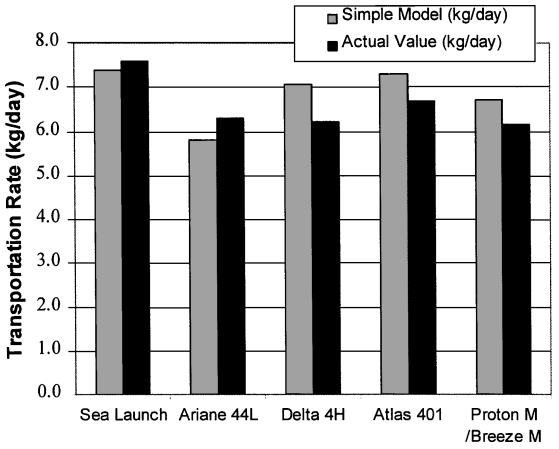

Fig. 16 Comparison of calculated EOR transportation rates vs simplified model (two SPT-140 thrusters).

user's guides, OBS performance is calculated assuming a Hohmann transfer, and EOR performance is calculated using the low-thrust optimizer already described. The transportation rates are mean values, calculated by averaging the performance of missions with durations varying from 10 to 140 days. The bars marked simple model in Fig. 16 show the transportation rate for each vehicle calculated using the most applicable multistage parametric model. Table 4 shows each vehicle's input parameters and the type of model applied. The two-stage model provides the best estimate for most launch vehicles. The only exception is the Sea Launch. In this case the detailed calculations show that the ΔV from the OBS is basically constant regardless of mission duration. In the three-stage model the effective I_{sp} of the launch vehicle is much lower than the actual I_{sp} of the chemical engine because of the structural mass penalty associated with the launch vehicle's upper stage.

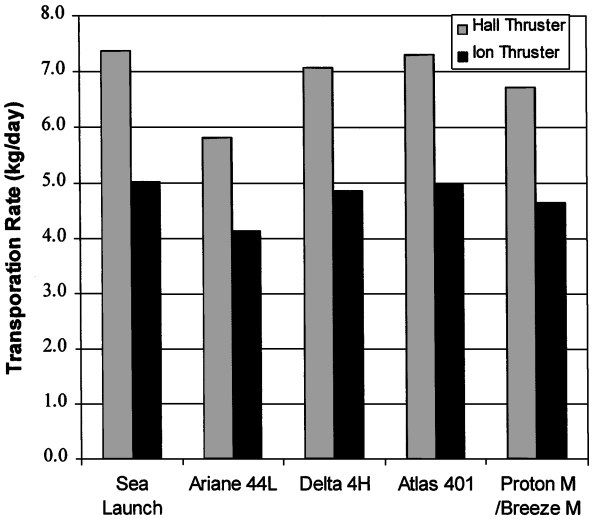

Fig. 17 Ion thruster vs Hall thruster performance for C-EOR missions.

In general, the match between the multistage model and the detailed calculations is within 9% with the exception of the Delta 4H, which shows a 13% error. Variations in accuracy are primarily caused by the linearization made in Eq. (11) and deviations in the optimized trajectories from the ideal two- and three-stage profiles. The Ariane in particular uses a trajectory with elements of both the two- and three-stage models, and so its actual performance is better than that calculated using the two-stage model. The primary source of error with the Delta 4 is the linearization. The high separated mass of the Delta 4 results in relatively long flight times for the trajectories shown in Fig. 13. The long flight times lead to significant deviations from the short time approximation. Better agreement can be achieved either by limiting the flight times considered or by using a more complex implicit model based on Eq. (9) to calculate the transportation rate.

One reason that the two-stage model applies to most launch vehicles is because we have chosen an all-chemical reference mission with a high separation inclination. When EOR ΔV is added to the mission profile, it can either displace ΔV from the launch vehicle or from the OBS. In the cases considered in this paper, the launch vehicle is already using a near-optimum trajectory, so that ΔV is displaced from the OBS. This makes the mission profile resemble a two-stage model. Large spacecraft might be unable to follow the baseline all-chemical mission because of tank size limits on the OBS. In these cases the launch vehicle flies a less optimized low inclination or supersynchronous trajectory. When EOR ΔV is added to these missions, the ΔV will be displaced from the launch vehicle instead of the OBS. The result is much closer to the three-stage model than the two-stage model and should result in higher transportation rates. Therefore, in cases where satellites today fly tank-limited trajectories, substantially higher transportation rates might be achievable than those shown in Fig. 16.

Using the parameters specified in Table 4, the two- and three-stage models can be used for system trade studies of different power and electric propulsion systems. The relative performance of two XIPS thrusters vs two SPT-140 thrusters operating at the same power level is shown in Fig. 17.

For C-EOR missions the SPT-140 Hall thrusters outperform the XIPS ion thrusters by about 30% or over 150 kg over 90 days because of their higher thrust level. This is to be expected, as the optimum specific impulse calculated using Eq. (14) is much closer to the operating point of an SPT-140 than it is to the operating point of a typical ion thruster.

Conclusions

A series of simple analytic models have been developed for combined chemical-electric orbit-raising missions (C-EOR). The models treat orbit raising as a series of chemical/electric stages and

have been used to derive a modified form of the rocket equation for a C-EOR mission. Expressions were derived for the transportation rate and optimum electric specific impulse for C-EOR missions. The results showed that the optimum electric I_{sp} depends primarily on the I_{sp} of the chemical thruster and on a mission planning efficiency η_v. Several different cases were considered, including two-stage, three-stage, variable-thrust-efficiency, and tank-capacity-limited cases.

A low-thrust-trajectory optimization model was combined with launch-vehicle performance data to derive fully optimized three-dimensional end-to-end C-EOR profiles for the Sea Launch, Ariane 4, Atlas V, Delta IV, and Proton launch vehicles. Based on our analysis, the following general conclusions can be drawn:

1) Using optimized trajectories, EOR transportation rates of 6 kg/day can be consistently achieved on most launch vehicles by a satellite with two SPT-140 thrusters. These rates assume ideal trajectories with no perturbation or steering losses and use nominal, published thruster performance values. Actual missions must take worst-case performance and losses into account when calculating C-EOR performance.

2) Optimum EOR starting orbits tend to increase in eccentricity as launch inclination increases. Because inclination is changed most efficiently when an orbit has a high apogee, launching from a high inclination leads to a relatively high EOR starting orbit. The Proton is an exception to this rule because it has a restartable upper stage that is used to raise perigee and change inclination prior to separation. The Proton's optimum EOR starting orbit is also elliptical but does not follow the same trend as launch vehicles without the restartable upper stage.

3) Optimum EOR starting orbits tend to increase in inclination as EOR duration increases.

4) On C-EOR missions transportation rate is a function of power available rather than payload mass or power to mass ratio.

Equation (13), which applies to short-duration EOR missions, shows that EOR transportation rate is primarily a function of thrust level and planning efficiency rather than separated mass or power to mass ratio. A consequence of this observation is that performance numbers calculated with a light version of a launch vehicle can also be applied to a heavy version of the same vehicle as long as it has a similar effective specific impulse and flies a similar trajectory.

Analytic two-stage and three-stage C-EOR models were applied to each launch vehicle. Modeling parameters were defined, and comparisons were made to detailed trajectory performance calculations. The results show the following.

5) A simple multistage C-EOR model can be used on short-duration missions to calculate performance on a variety of launch vehicles within an accuracy of about 9%. An exception is the Delta 4, where long flight times result in an accuracy of only 13%.

The parametric model is a good tool for system level analysis of electric orbit raising missions and for trades involving different types of electric thrusters, power levels, and thrust levels. For instance, the multistage model has been used to compare the performance of Hall and Ion thrusters for orbit raising. The result shows the following:

6) SPT-140 Hall thrusters can provide EOR transportation rates 30% higher than XIPS ion thrusters operating at the same input power level. This conclusion is consistent with calculations showing that Hall thrusters operate near the optimum specific impulse level for electric orbit raising.

Taken together, the results demonstrate the capability to optimize electric orbit raising missions to geostationary orbit (GEO) with major commercial launch vehicles. This is an important and enabling step to the use of fully optimized C-EOR trajectories for orbit raising on commercial satellite missions. The results also show how a simple analytic model can be used to calculate the approximate performance of and optimum I_{sp} for C-EOR missions to GEO.

Acknowledgments

Thanks to Steve Snyder and Walter Gelon at Space Systems/Loral for their help with the derivation of Eqs. (9) and (14) and general insight into the electric orbit raising problem, respectively.

References

[1]Randolph, T., "Overview of Major U.S. Industrial Programs in Electric Propulsion," AIAA Paper 99-2160, July 1999.

[2]Killinger, R., Kukies, R., Surauer, M., Saccoccia, G., and Gray, H., "Final Report on the ARTEMIS Salvage Mission Using Electric Propulsion," AIAA Paper 2003-4546, July 2003.

[3]Kim, V., Popov, G., Tikhonev, Garkusha, V., and Murasko, V., "Modern Trends of Electric Propulsion Activity in Russia," International Electric Propulsion Conf., Paper 99-004, Oct. 1999.

[4]Stuhlinger, E., *Ion Propulsion for Space Flight*, 1st ed., McGraw–Hill, New York, 1964, pp. 101–108.

[5]Burton, R., and Wassgren, C., "Time-Critical Low-Thrust Orbit Transfer Optimization," *Journal of Spacecraft and Rockets*, Vol. 29, No. 2, 1992, pp. 286–288.

[6]Spitzer, A., "Near Optimal Transfer Orbit Trajectory Using Electric Propulsion," American Astronomical Society, Paper 95-215, Feb. 1995.

[7]Pollard, J. E., "Evaluation of Low-Thrust Orbital Maneuvers," AIAA Paper 98-3486, July 1998.

[8]Sackett, L., and Edelbaum, T., "Effect of Attitude Constraints on Solar-Electric Geocentric Transfers," *Journal of Spacecraft and Rockets*, Vol. 13, No. 3, 1976, pp. 174–179.

[9]Ilgen, M., "A Hybrid Method for Computing Optimal Low Thrust OTV Trajectories," American Astronomical Society, Paper 94-129, Feb. 1994.

[10]Oleson, S. R., and Myers, R. M., "Launch Vehicle and Power Level Impacts on Electric GEO Insertion," AIAA Paper 96-2978, July 1996.

[11]Kaufman, H. R., and Robinson, R. S., "Electric Thruster Performance for Orbit-Raising and Maneuvering," *Orbit Raising and Maneuvering Propulsion: Research Status and Needs*, edited by L. H. Caveny, Vol. 89, Progress in Astronautics and Aeronautics, AIAA, New York, 1984, pp. 303–326.

[12]Snyder, J. S., Randolph, T., Oh, D., Sauer, B., and Fischer, G., "System-Level Trade Studies of a Dual-Mode SPT for Geosynchronous Communications Satellites," International Electric Propulsion Conf., Paper 01-173, Oct. 2001.

[13]Oleson, S. R., "Mission Advantages of Constant Power, Variable I_{sp} Electrostatic Thrusters," AIAA Paper 2000-3413, July 2000.

[14]Gnizdor, R., Kozubsky, K., Maslennikov, N., Murashko, S., Pridannikov, S., and Kim, V., "Performance and Qualification Status of Multimode Stationary Plasma Thruster SPT-140," International Electric Propulsion Conf., Paper 99-090, Oct. 1999.

[15]de Gris, K., Meckel, N., Callis, G., Greisen, D., Hoskius, A., King, D., Wilson, F., Werthman, L., and Khayms, V., "Development and Testing of a 4500 Watt flight Type Hall Thruster and Cathode," International Electric Propulsion Conf., Paper 01-011, Oct. 2001.

[16]Kimbrel, M. S., "Optimization of Electric Propulsion Orbit Raising," M.S. Thesis, Aeronautics and Astronautics, Massachusetts Inst. of Technology, Cambridge, MA, June 2002.

[17]"Sea Launch User's Guide," Rev. B, Boeing Commercial Space Co., Seattle, WA, July 2000.

[18]Stechman, C., Woll, P., Fuller, R., and Colette, A., "A High Performance Liquid Rocket Engine for Satellite Main Propulsion," AIAA Paper 2000-3147, July 2000.

[19]Goebel, D., Martinez-Lavin, M., Bond, T., and King, A., "Performance of XIPS Electric Propulsion in On-Orbit Station Keeping of the Boeing 702 Spacecraft," AIAA Paper 2002-4348, July 2002.

[20]"Ariane 4 User's Manual," No. 2, Arianespace, Evry, France, Feb. 1999.

[21]"Atlas Launch System Mission Planner's Guide, Atlas V Addendum," Rev. 8, International Launch Services, San Diego, CA, Dec. 1999.

[22]"Delta IV Payload Planners Guide," Ver. 2000, Boeing Co. (Delta Launch Services), Huntington Beach, CA, Oct. 2000.

[23]"Proton Launch System Mission Planner's Guide," Issue 1, Rev. 5, International Launch Services, LKEB-9812-1990, McLean, VA, Dec. 2001.

[24]Randolph, T., and Oh, D., "Economic Benefit Analysis of Chemical-Electric Orbit Raising Missions," AIAA Paper 2002-1980, May 2002.

J. A. Martin
Associate Editor